symmetry

MDPI

Article

In Silico Comparison of Quantum and Bioactivity Parameters of a Series of Natural Diphenyl Acetone Analogues, and In Vitro Caco-2 Studies on Three Main Chalcone Derivatives

Amalia Stefaniu [1], Georgeta Neagu [1], Adrian Albulescu [1,2], Nicoleta Radu [3,4] and Lucia Camelia Pirvu [1,*]

[1] National Institute of Chemical Pharmaceutical Research and Development, ICCF-Bucharest, 112 Vitan, 031299 Bucharest, Romania; astefaniu@gmail.com (A.S.); georgetaneagu2008@gmail.com (G.N.); rockady@gmail.com (A.A.)
[2] Stefan S. Nicolau Institute of Virology, 285 Mihai Bravu, 030304 Bucharest, Romania
[3] Biotechnology Faculty, University of Agronomic Sciences and Veterinary Medicine of Bucharest, 59 Marasti, District 1, 011464 Bucharest, Romania; nicoleta.radu@biotehnologii.usamv.ro
[4] Biotechnology Department, National Institute of Chemistry and Petrochemistry Research and Development, 202 Splaiul Independentei, District 6, 031299 Bucharest, Romania
* Correspondence: lucia.pirvu1@gmail.com

Abstract: This paper aims to compare the in silico and in vitro properties of a series of diphenyl acetone derivatives, specifically six chalcone analogues, namely benzophenone, chalcone, phloretin, phloridzin, nothofagin and 4-methylchalcone. The in silico studies were conducted using the Spartan'14 mechanistic program to perform a comparative analysis of the molecular, quantum and bioactivity parameters of the six analogues under study. The in vitro MTS studies were designed to investigate the cytotoxic and anti-proliferative effect of the reference substances (r.s.) of three main chalcone derivatives in nature, namely phloretin, phloridzin and 4-methylchalcone, on the Caco-2 cell line. Overall, the in silico results foremost suggested the potential of phloretin to traverse the blood–brain barrier, and the abilities of phloridzin and nothofagin to act as broad cell enzyme inhibitors; the in vitro results demonstrated that phloretin and 4-methylchalcone have the potential to induce both cytotoxic and anti-proliferative effects, depending on their concentration level: the antiproliferative effects were noticed in the interval from 1 to 50 µg of r.s. per sample, while the cytotoxic effects were noticed from 1 to 50 µg of r.s. per sample in the case of 4-methychalcone, and at 50 µg of r.s. per sample in the case of phloretin. Phloridzin did not affect the viability of the Caco-2 line.

Keywords: chalcone analogues; in silico quantum; bioactivity and docking studies; TNKS1 target; in vitro studies; MTS method; cytotoxicity and antiproliferative assays; Caco-2 cells

Citation: Stefaniu, A.; Neagu, G.; Albulescu, A.; Radu, N.; Pirvu, L.C. In Silico Comparison of Quantum and Bioactivity Parameters of a Series of Natural Diphenyl Acetone Analogues, and In Vitro Caco-2 Studies on Three Main Chalcone Derivatives. *Symmetry* **2024**, *16*, 1383. https://doi.org/10.3390/sym16101383

Academic Editor: György Keglevich

Received: 13 September 2024
Revised: 11 October 2024
Accepted: 14 October 2024
Published: 17 October 2024

1. Introduction

The benzene nucleus and its substituted derivatives (hydroxyl, carboxyl, methoxyl, etc.) are the basis of countless natural and synthetic compounds, many of which have important pharmacological activities and certain human health benefits.

More complex variants, such as those obtained by condensing multiple benzene nuclei or derivatives through the interposition of alkene, polyene, keto, amino groups, or by adding heterocyclic groups containing O,N,S heteroatoms, often deepen one or more pharmacological effects. However, the more complex the natural or new-fashioned active molecules, the more complex the testing of their safety for practical use. For example, although planar lipophilic and planar symmetrical lipophilic molecules are known to be highly effective drug compounds, they have the ability to switch the dipole moment of the cell membranes, causing chaotic effects or even disrupting the lipid layer, which may lead to the death of the cells [1–4].

As is well known, symmetrical molecules achieve maximum interaction potency and effectiveness when combined with molecular targets that also exhibit symmetrical conformation; thus, symmetrical molecules are highly effective in targeting active proteins with symmetrical sub-unit arrangements or proteins that display a symmetrical arrangement of the amino acids in their binding pockets [5,6].

The concept of the superiority of symmetrical drugs for symmetrical targets is based on the notion of the dyad axis, which refers to "the best axis which gives the lowest root mean square deviation between each atom of a pair and the 180° rotated position of its partner" [7]); by calculating the best dyad axis of a drug molecule in relation to its interaction partner (the binding site in the active protein), the development of highly effective drug–receptor couple force molecular pairs has become possible.

An example of a symmetrical, non-polar, natural drug molecule is benzophenone (Figure 1a), a diphenyl ketone compound considered a fundamental and ubiquitous structure in pharmaceutical chemistry, thus being the basis of numerous active compounds [8]. Benzophenone is naturally produced by certain microorganisms (fungi) and can also be found in green plants and some edible fruits, such as grapes [9].

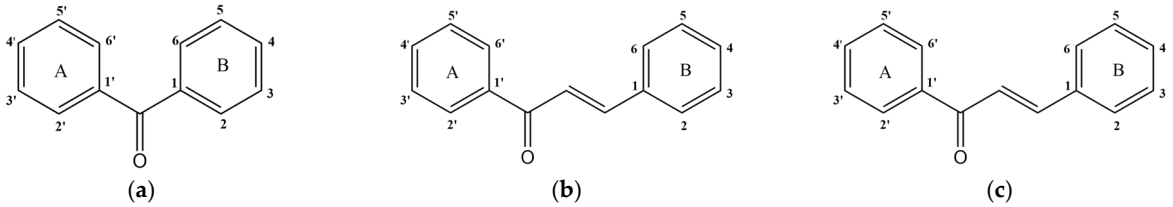

Figure 1. Structures of bezophenone core (**a**) stilbene core (**b**), and chalcone core (**c**).

Stilbene (Figure 1b) is another example of a symmetrical, non-polar, natural drug molecule of high pharmacological interest. Interposing a vinyl group between the benzophenone nuclei or a ceto group between the stilbene nuclei results in a new chemical analogue: 1,3-diphenylprop-2-en-1-one. This analogue forms the basis of some of the most active subclasses in the green plant and polyphenol series, namely, the chalcone (Figure 1c) series.

The most well-known chalcone-type compounds in nature are phloretin (aglycone) and its *O*-glucoside derivate, phloridzin. Phloretin and phloridzin belong to the class dihydrochalcones and can be found in many edible fruits and medicinal herbs. For example, the content of phloridzin in apples, strawberries, plums and apricots ranges from 0.5 to 3 mg per 100 g wet weight/(WW), while Mexican oregano has the highest content of phloridzin in nature, at 136 mg % (WW) [10].

In vitro and in vivo studies on different chalcone derivatives, particularly the phloretin aglycone, have shown their ability to induce a plethora of biological effects. The most noteworthy are antimicrobial, antifungal and antiparasitic effects, cytotoxic, antitumor, antiproliferative, angiogenic and antimetastatic effects, antidiabetic and antiobesity effects, antioxidant and anti-inflammatory effects, cardioprotective, vasculoprotective, hepatoprotective and neuroprotective effects, effects on skin conditions, and even immunosuppressant effects [11–15]. However, some studies have also reported significant harmful effects [3,4,12].

These harmful effects have specifically been attributed to the planar non-polar structure of the phloretin, which can induce changes in the membrane dipole potential, potentially causing the disruption of the membrane permeability and cell homeostasis.

Studies have confirmed that phloretin aglycone can modify the dipole potential of the lipid bilayers by bonding the cholesterol-rich domains, thereby altering the permeability of the cell membrane for various compounds and further disrupting cellular homeostasis [3,4]. Phloretin is in fact an example of a so-called PAIN molecule (Pan-Assay compound), meaning a molecule that has the ability to interfere with compound bioassays through different molecular mechanisms [16].

However, due to the introduction of a *C*-glucoside moiety into the phloretin molecule (specifically at position 3′ of ring A) resulting in a more polar analogue, namely nothofagin, the new chalcone derivative is not able to alter the membrane dipole potential of cells [14,17]. Yet, phloridzin, the *O*-glucoside derived at position 2′ of ring A and in fact the major chalcone derivate in green plants, also showed harmful effects in the in vivo model; the harmful effects were seen in either muscle mass and strength, or in osteoporotic changes in the studied mouse groups [18].

Apart from these, studies have revealed that both phloretin and phloridzin glucoside exhibit very low bioavailability (8.67%) in humans [14,19–21]; as is well known, phloridzin is metabolized into its aglycone, phloretin, and glucose unit with the help of lactase hydrolase, an intestinal enzyme involved in the metabolism of many other flavonoids derivates. Lactase hydrolase is found in the epithelial brush border membrane of the small intestine. Thus, similar to other flavonoid derivates, the bioavailability and the bioactivity of *O*-glucoside derivatives are those of aglycones. Research also shows that the intestinal permeability of the phloretin aglycone decreases as the pH increases, therefore following this absorption pattern: colon > duodenum > jejunum > ileum [14]. Pharmacokinetic in vitro and in vivo studies have also demonstrated that microemulsion, liposome and self-nanoemulsion formulations result in a 4-to 7-fold increase in bioavailability [14,19,22–26], as well as in a reduction in the membrane disruption effects [14]. Furthermore, the 4-methylchalcone derivative, the main chalcone metabolite in humans, along with many other methyl analogues obtained through chemical synthesis have shown lower toxicity in normal cells and/or stronger activity in cancer cells, and improved pharmacokinetic profiles too [14,19,22–26]; as a result, interest in their green synthesis has increased [27–31].

Considering all these aspects, to enhance our knowledge and valorization of the chalcone analogues in the current plant-derived medicines, the present study aimed to analyze the in silico, molecular, quantum and bioactivity parameters of six chalcone analogues from green plants, namely benzophenone, chalcone, phloretin, nothofagin, phloridzin and 4-methylchalcone; docking studies were performed on a molecular target for the tumorigenesis process and particularly for colon cancer in humans, named TNKS1. In silico studies were followed by an in vitro comparison of the anti-proliferative potency of phloridzin (the major glucoside form present in the green plants), phloretin (the aglycone form released by the specialized enzymes in the small intestine) and 4-methylchalcone (the metabolized form that results after passing the intestinal metabolism) on Caco-2 cells. The choice of using Caco-2 cells is based on the fact that chalcone derivatives are very active natural compounds when they come into direct and long-term contact with the intestinal cells during the digestion process in humans; therefore, the results could be of interest for the chemical pharmaceutical and food supplement industries In vitro studies were performed on the reference substances (r.s.) solubilized in 50% ethanol, at concentration levels ranging from 1 to 50 μg of test chalcone per sample, therefore suggesting the daily intake of humans.

2. Materials and Methods

2.1. In Silico Molecular, Quantum and Bioactivity Parameters Studies

The structures of the six investigated compounds (benzophenone, chalcone, phloretin, phloridzin, nothofagin and 4-methylchalcone) were first drawn and converted into 3D. Their lower energy conformers were obtained by energy minimization using the Merck molecular force field (MMFF) [32], by means of Spartan software, Wavefunction, Inc. Irvine, CA, USA [33]. The Density Functional Theory [34] algorithm and basis set were settled to give good accuracy predictions for the molecular property calculations; the B3LYP hybrid functional [35] with the basis set 6-311G (d,p) was used [36], as demonstrated by previous investigations [37–39]. Specifically, the computations were performed for the equilibrium geometry at ground state in gas, without any solvent corrections. The purpose of the property computations was to achieve a comparative analysis of several major molecular features and structural descriptors, including the molecular weight, total surface, volume, polar surface area (PSA), water–octanol partition coefficient (logP), dipole moment,

polarizability, ovality, number of hydrogen bond donors (HBDs) and acceptors (HBAs). These descriptors suggest their potential use as new natural medicines. In addition, to gain insights on the chemical reactivity of the investigated structures, the quantum descriptors related to the chemical reactivity were also calculated; these descriptors included the highest Occupied Molecular Orbital (HOMO) and the Lowest Unoccupied Molecular Orbital (LUMO), the Frontier Molecular Orbitals (FMOs) energy gap (ΔE), the ionization potential (I), the electron affinity (A), the chemical hardness (η), the electronegativity (χ), the chemical potential (μ), the chemical softness (σ), the electrophilicity (ω), and the nucleophilicity (ε).

The bioactivity scores and quantum parameter prediction computation of the six compounds under investigation were obtained using the Molinspiration Cheminformatics free web services, Slovensky Grob, Slovakia [40]. Specifically, the ability of the six chalcone analogues to inflect the protein-coupled receptor (GPCR) ligand and nuclear receptor ligand were analyzed, as well as the ion channel, kinase, protease and cell enzyme activities.

2.2. In Silico Docking Studies

Molecular docking studies were performed through CLC Drug Discovery Workbench (QIAGEN, Aarhus, Denmark) software in order to investigate the potential inhibitory effect of the six chalcone analogues under study upon the activity of one important molecular target for colon cancer development in humans, the human tankyrase 1 (TNKS1) enzyme. According to the available data [41–43], the catalytic domain of the human tankyrase 1 is implicated in the oncogenesis process by the Wnt/β-Catenin signaling pathway, which is particularly responsible for the regeneration of the intestinal epithelial cells and the development and progression of colorectal cancer. The PDB entree 4W6E, corresponding to the TNKS1 target, in complex with the native inhibitor encoded Co-crystallized 3J5A [43] was retrieved from the Protein Data Bank (https://www.rcsb.org, accessed on 1 January 2020). The TNKS1 preparation consisted of removing the co-factor (Zn ion) and the water molecules, protonation, and setting up the binding site and binding pocket at 140.29 $Å^2$. The ligand's preparation was achieved by energy minimization using the Spartan'14 software program from Wavefunction, Inc., Irvine, CA, USA [33]; validation was performed by re-docking the native ligand, after which the interactions of the test ligands in complex with the catalytic domain of TNKS1 were determined by docking. More detailed information can be found in the authors' previous studies [44,45].

2.3. In Vitro Studies

In vitro pharmacological studies were performed on Caco-2 cells (ATCC, HTB-37) following the protocol described by the CellTiter 96AQueous One Solution Cell Proliferation Assay Promega Corporation (Madison, WI, USA) for the cytotoxicity and anti-proliferative MTS assays, respectively [46]. Essentially, the MTS Promega protocol is based on the selective ability of the viable cells in culture to reduce the tetrazolium component of the MTS salt [3-(4,5-dimethylthiazol-2-yl)-5-(3-carboxymethoxyphenyl)-2-(4-sulfophenyl)-2H-tetrazolium] to a purple-colored formazan; the resulting colored formazan in the medium can then be measured at 492 nm. Briefly, the MTS cytotoxicity and anti-proliferative assays' setup consists of the cells being exposed to the test/control samples when a "semiconfluent" or a "sub-confluent"-type cell type culture is achieved, meaning 70% cell proliferation versus 30% cell proliferation, respectively. MTS studies were performed on three main chalcone derivatives in nature: phloretin (by Molekula GmbH, München, Germany), phlorizin hydrate (by TCI, Tokio Chemical Industry, Tokio, Japan), and 4-methylchalcone (by Sigma Aldrich, Merck Darmstadt, Germany); these were presented as reference substances (r.s.) prepared as stock solutions of 1 mg/1 mL of 50% ethanol (w/v). The three reference substances (r.s.) were further prepared as a six-point dilution series in the interval from 1 to 50 μg/mL of test sample, also using 50% ethanol. The same dilution series were used for the positive control series using 50% ethanol, and for the negative control series using Caco-2 cell growth medium supplemented with FBS (from Merck Sigma-Aldrich, Saint

Louis, MO, USA distributor in Romania). Briefly, after reaching the Caco-2 cell culture confluence established by the two Promega protocols, the cells were detached from the flask with Trypsin-EDTA; the resulting suspensions were centrifuged at 2000 rpm for 5 min, after which they were re-suspended in the Caco-2 growth medium. The resulting cells were further seeded in 96-well plates at a density of 4000 cells per well, in 200 µL of Caco-2 growth medium. After reaching the Caco-2 cell culture confluence established (70% and 30%, respectively), each one test sample in the three series, as well as the positive and the negative control sample series at each one dilution point in the series, were applied to the Caco-2 cell culture in triplicate (n = 3). After 20 and 44 h of Caco-2 cell exposure to the test and positive/negative control series, the culture medium was removed. The cells were incubated with MTS solution for another two hours and, after that, the viability of the adherent cells was determined by evaluating the absorbance of the solutions at 492 nm (BMR-100 Microplate Reader, Boeco, Germany). The Optical Densities (O.D.) at 492 nm, as well as the viability percentages of the test series against the positive control series along the concentration series (mean values, n = 3), were computed for their statistical significance (Student "*t*" test). The notation (*) represents results without statistical significance and $p > 0.05$; the notation (**) represents results with statistical significance and $0.05 < p < 0.01$; and the notation (***) represents results with statistical significance and $p < 0.01$.

3. Results

3.1. In Silico Studies Results

Quantum Bioactivity Parameters Computation of the Six Test Compounds

The first part of the investigation aimed to compare the main molecular properties (molecular weight, area, volume, polar surface area, water–octanol partition coefficient, dipole moment, polarizability, ovality, the number of hydrogen bond donors and acceptors) of the six test compounds under investigation: benzophenone, chalcone, phloretin, nothofagin, phloridzin and 4-methylchalcone.

Their chemical structures are shown in Figure 2.

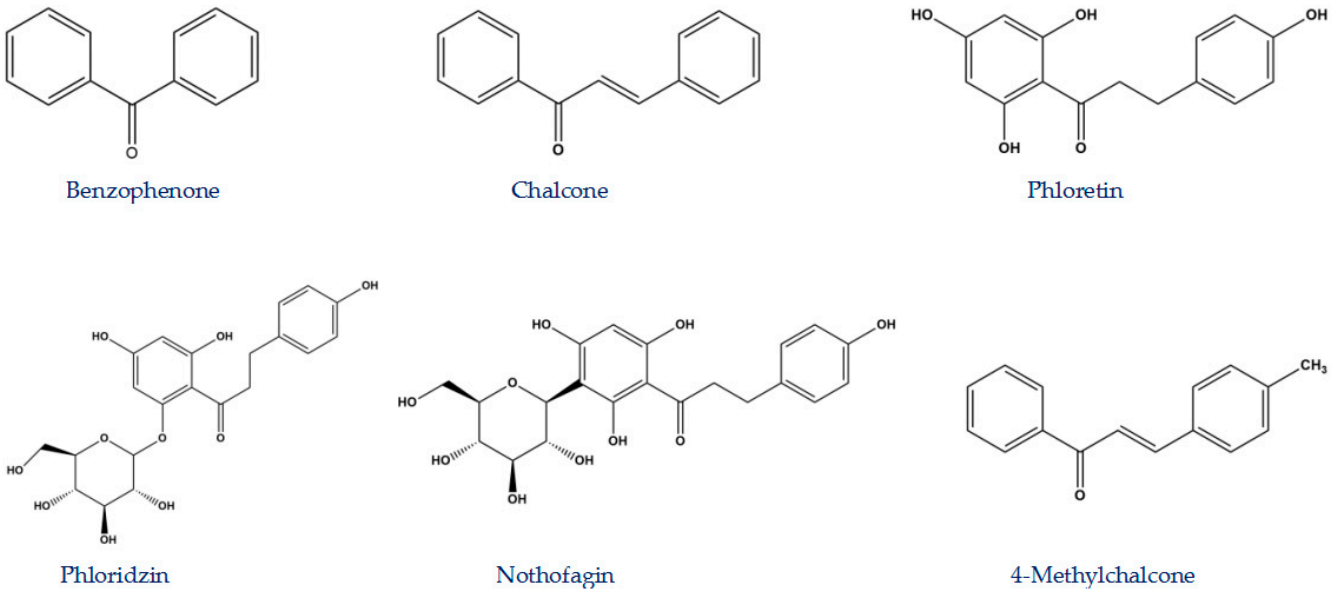

Figure 2. Chemical structure of the six chalcone analogues.

Table 1 shows the data on the molecular properties of the six chalcone analogues under study, computed using DFT/B3LYP functional with the 6-311(d,p) basis set.

Table 1. The main molecular properties of the six chalcone analogues in the study.

Test Compounds	MW	Area	Volume	PSA	log*P*	Dipole Moment	Polarizability	Ovality	HBD	HBA
Benzophenone	182.22	215.35	203.24	14.069	3.24	3.01	56.69	1.29	0	1
Chalcone	208.260	251.74	236.07	13.761	3.76	3.09	59.53	1.36	0	1
Phloretin	274.272	293.31	269.08	90.979	2.05	6.6	62.0	1.46	1	5
Phloridzin	436.413	431.51	405.89	153.365	0.21	7.26	73.12	1.63	7	10
Nothofagin	436.413	416.69	399.79	151.334	−0.58	8.42	72.76	1.59	7	10
Methylchalcone	222.287	265.93	253.63	14.379	4.25	3.75	60.91	1.37	0	1

Where: MW—molecular wight (Da), area (Å^2), volume (Å^3), PSA—polar surface area (Å^2), log*P*—water-octanol partition, dipole moment (Debye), polarizability (10^{-30} m^3), ovality, HBDs—number of hydrogen bond donors and HBAs—number of hydrogen bond acceptors.

As is well known, the area (A) and volume (V) of the compounds are in close relation with the molecular weight (MW), while the polar surface area (PSA) generally depends on the number and configuration of the hydroxyl groups in a compound, and other polar hetero-atoms or functional groups, respectively. The PSA value is also known as a measure of the presence of oxygen sp^3 or sp^2 hybridization in a molecule; therefore, it increases with the number of hydroxyl groups in the molecule. The PSA value estimates the ability of a molecule to pass through the hydrophilic or hydrophobic medium, too; thus, the higher the PSA value, the more hydrophilic the molecule.

The logarithm of the water–1-octanol partition coefficient, Log*P*, is an indicator of the lipophilicity/hydrophilicity balance of a molecule, being in fact the widely used molecular descriptor for the prediction of the oral bioavailability of biologically active compounds in humans; Log*P* is estimated according to the method of Ghose, Pritchett and Crippen [47], who used refined atomic parameters to predict the octanol–water partition coefficient by taking into account 125 compounds and obtaining a good correlation given by good standard deviation and correlation coefficients. As was stated [48–52], a negative log*P* indicates the compound's affinity for the aqueous phase; a log*P* value near to zero means that there is equal affinity for the lipid and the aqueous phases; a positive value for log*P* suggests a higher affinity for the lipid phase than the aqueous phase; log*P* = 1 means a 10:1 ratio of the compound partitioning between the organic and aqueous phases; a log*P* value close to 2 indicates the ability of the compound to cross the blood–brain barrier; a log*P* value in the interval from 1.35 to 1.8 describes a compound targeting the common oral-intestinal absorption in humans; and a log*P* higher than 5 describes a compound able to undergo sublingual absorption in humans.

Furthermore, the dipole moment and the polarizability are both closely related to the electronic structure of the compound; therefore, they can estimate the reactivity and the potential bonding to a molecular target [53,54]. Since it combines area, volume and PSA three-dimensional information, the ovality index offers cumulative information about the investigated molecule; the ovality index also represents the deviation from the spherical shape, which corresponds to an ovality index equal to 1. Hereby, the higher a value is, the further it is from the shape of a sphere; therefore, it also indicates an increase in the linearity of the molecule. It must be noted that studies on 16 phenolic compounds in the series of flavonoid derivatives indicated that their ovality index is related to their ability to act as trypsin and trypsin-like enzyme inhibitors [55]; these data are very useful for the health and dietary and food supplement industries.

Finally, the counts of the hydrogen-bond donors (HBDs) and acceptors (HBAs) are based on the atomic connectivity following special cases for common organic functional groups; they are related to the potency of a molecule to bind a specific molecular target, and stand as pharmacological filters when discussing the Lipinsky rule of five [56].

Altogether, the results in Table 1 suggest the high probability of phloretin crossing the blood–brain barrier in humans, as well as the capability of 4-methylchalcone to undergo sublingual absorption. Benzophenonone, phloridzin and nothofagin suggest intestinal

metabolism and absorption in humans. Cumulatively, phloridzin and nothofagin suggest similar bioavailability and formulation needs for humans.

Figure 3 compares the main molecular properties of the four chalcone derivatives under study: differences between the polar and less polar chalcone derivatives in the study in terms of the logP, dipole moment, HBAs and HBDs can be observed. These areas anticipate the lipophylicity, hydrophilicity and formulation needs of phloretin, phloridzin, nothofagin and 4-methylchalcone for their usage in humans.

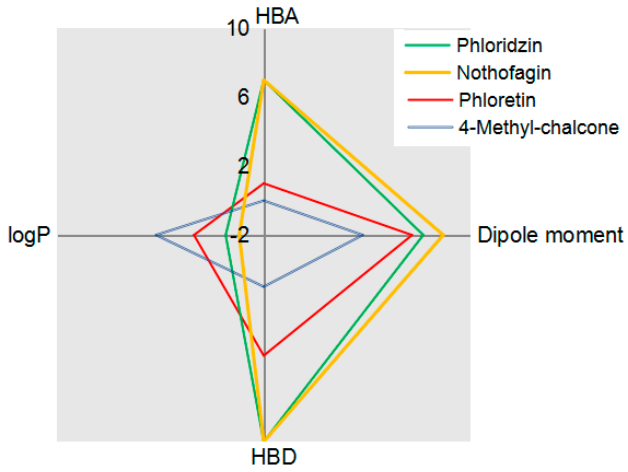

Figure 3. The abstraction of the main molecular properties: log*P*, dipole moment, HBA and HBD.

Table 2 resumes the bioactivity scores of the six test compounds against the six cell modulators in the eukaryotes: the G protein-coupled receptors (GPCRs), the ion channel, the kinase inhibitor, the nuclear receptor, the protease and the enzyme inhibitor activities. As is well known, a high bioactivity score indicates the greater probability of the test molecule modulating/impacting the molecular target subjected; in accordance with other predictive studies analyzed [57,58], the molecules that exhibit bioactivity scores more than 0 are highly active; the molecules with bioactivity scores between −5.0 and 0.0 are moderately active; and the molecules with bioactivity scores less than −5 are inactive.

Table 2. The bioactivity scores of the six chalcone analogues against the six cell modulators.

Test Compounds	GPCR Ligand	Ion Channel Modulator	Kinase Inhibitor	Nuclear Receptor Ligand	Protease Inhibitor	Enzyme Inhibitor	No. of Values > 0
Benzophenone	−0.47	−0.10	−0.46	−0.39	−0.72	−0.14	0
Chalcone	−0.43	−0.18	−0.66	−0.51	−0.60	−0.12	0
Phloretin	0.03	0.19	−0.17	0.27	−0.03	0.28	4
Phloridzin	0.17	0.17	−0.09	0.26	0.14	0.44	5
Nothofagin	0.21	0.20	−0.06	0.23	0.19	0.51	5
4-Methylchalcone	−0.41	−0.26	−0.61	−0.46	−0.59	−0.17	0

As a general observation, the chalcone analogues investigated are moderate to highly active natural molecules, and are able to impact the general function of the eukaryotic cells; the compounds with the lowest PSA values, specifically benzophenone, chalcone and 4-methylchalcone, have the lowest ability to influence the molecular targets selected; the compounds phloridzin and nothofagin both suggest a high ability to impact the cell enzyme activity and the nuclear receptor activity of the eukaryotic cells; and phloretin is less active than its glucoside derivatives. Similar to other polyphenolic species [39,55], chalcone derivatives appear to also potentially interfere with the activity of the enzymes in humans; therefore, they should be paid attention to in digestive diseases.

Table 3 presents the quantum chemical reactivity parameters of the six chalcone derivatives in the study, computed with the DFT/B3LYP/6-311 (d,p) method for the lowest energy conformers. These values are the basis for the prediction of other chemical reactivity descriptors derived from relationships established by Koopmans' theory [59–61], together providing information about charge transport within the molecule.

Table 3. Quantum chemical reactivity parameters of the six chalcone analogues.

Parameter	Formula	Benzo Phenone	Chal Cone	Phlore Tin	Phlori Dzin	Notho Fagin	4-Methyl Chalcone
E_{HOMO}		−6.87	−6.56	−5.91	−5.85	−5.96	−6.31
E_{LUMO}		−1.94	−2.35	−0.85	−0.84	−1.55	−1.92
ΔE	$\Delta E = E_{HOMO} - E_{LUMO}$	4.93	4.21	5.06	5.01	4.41	4.39
I	$I = -E_{HOMO}$	6.87	6.56	5.91	5.85	5.96	6.31
A	$A = -E_{LUMO}$	1.94	2.35	0.85	0.84	1.55	1.92
η	$\eta = (I - A)/2$	2.465	2.105	2.530	2.505	2.205	2.195
χ	$\chi = (I + A)/2 = -\mu$	4.405	4.455	3.380	3.345	3.755	4.115
μ	$\mu = -(I + A)/2$	−4.405	−4.455	−3.380	−3.345	−3.755	−4.115
σ	$\sigma = 1/\eta$	0.4056	0.4750	0.3952	0.3992	0.4535	0.4556
ω	$\omega = \mu^2/2\,\eta$	3.936	4.714	2.258	2.233	3.197	3.857
ω^+	$\omega^+ = (I + 3A)^2/16\,(I - A)$	2.0415	2.7498	0.8840	0.8739	1.5954	2.0741
ω^-	$\omega^- = (3I + A)^2/16\,(I - A)$	6.4465	7.2049	4.2640	4.2189	5.3504	6.1891
ε	$\varepsilon = 1/\omega$	0.254	0.212	0.443	0.448	0.313	0.259

Where: E_{HOMO}—energy of the HOMO orbital (eV); E_{LUMO}—energy of the LUMO orbital (eV); ΔE—FMOs energy gap (eV); I—ionization potential (eV); A—electron affinity (eV); η—chemical hardness (eV); χ—electronegativity (eV); μ—*chemical potential* (eV^{-1}); σ—chemical softness (eV^{-1}); ω—electrophilicity; ε—nucleophilicity.

Accordingly, in a comparison of the quantum parameters of the six chalcone analogues under study, we first suggested a high similarity between benzophenone, chalcone and 4-methylchalcone, and between phloretin and phloridzin; nothofagin differs in its analogues mainly in terms of electron affinity and electrophilicity. These data suggest that polarity, in fact the number and the position of the hydroxyl groups at the benzene nucleus, is the basis of the similarity between the quantum reactivity parameters in an analogue series.

The number and position of the hydroxyl groups in the benzene nucleus also are at the basis of antioxidant activity. Nevertheless, the antioxidant potency of the analogue's series cannot be predicted using nucleophilicity and electrophilicity values. According to previous studies [62], "oxidants are electrophiles that take one or two electrons from a nucleophile, without forming an adduct" and "reductants are nucleophiles that give one or two electrons to and oxidant, without forming an adduct"; the antioxidants (reactive oxygen scavengers) are "nucleophilic reductants that directly react with oxidants, thus preventing the oxidation of a third molecule". This way, the antioxidant activity is, in fact, a complex interplay of nucleophilic and electrophilic reactions and, therefore, cannot be predicted based on the quantum and energy parameters in silico.

Finally, the HOMO-LUMO energy gap (ΔE) (see Figure S1A–G) gives indications about the stability of the series analogues; the larger the difference between the HOMO-LUMO frontier orbital energy (ΔE), the more stable the individual molecules; in particular, ΔE for the six series analogues corresponds to 4.39–5.06 eV, suggesting the high stability of the chalcone analogues. Also, a high HOMO energy in a compound suggests the greater probability of the respective molecule undergoing an electrophilic attack; therefore, by comparison, phloretin and phloridzin are the most stable compounds in the series, while the chalcone core is the most potentially reactive species in the series.

Table 4 shows the results of docking studies on the TNKS1 (PDB ID: 4W6E) molecular target. Figure S2 (see the Supplementary Materials) shows the interactions between the amino acids in the active pocket of TNKS1 and the native ligand and chalcone analogues, respectively.

Table 4. Results of a molecular docking study on TNKS1 (PDB ID: 4W6E, chain A) [43].

Test Ligand	Interacting Group/4W6E, Chain A	Hydrogen Bonds: Å	Score/RMSD
The native ligand (Co-crystallized 3J5A)	MET1207, GLY1206, ILE1204, GLU1291, ALA1202, TYR1203, HIS1201, TYR1213, PHE1214, ALA1215, PHE1183, LYS1220, HIS1184, ILE1228, GLY1185, TYR1224, SER1185, PHE1188, PRO1187, LY1227, SER1121, ALA1290.	O1 sp^3–Osp^2 GLU1291: 3.393 O1 sp^3–Osp^2 GLU1291: 3.250 O sp^2–Osp^3 SER1221: 2.778 O sp^2–Nsp^2 GLY1185: 2.895	−104.15/0.16
Benzophenone	PHE1188, PRO1187, VAL1225, GLY1185, TYR1224, HIS1184, PHE1183, SER1221, ILE1228, ALA1215, PHE1214, TYR1203, GLU1291, LYS1220, TYR1213	No bonds	−59.52/0.03
Chalcone	ILE1228, TYR1203, GLY1227, PRO1187, PHE1188, ALA1202, SER1186, GLY1185, HIS1184, PHE1183, PHE121, TYR1213, GLY1227, ALA1215, SER1221, ALA1290, ALA1215, LYS1220, GLY1291, PHE1214, ALA1290	O0 sp^2–Nsp^2 HIS1184: 3.261	−69.30/0.03
Phloretin	ALA1290, GLU1291, TYR1292, GLY1211, ALA1202, TYR1203, ILE1212, TYR1213, PHE1214, ALA1215, GLY1216, LYS1220, SER1221, HIS1184, PHE1183, ILE1228, SER1186, PHE1188, PRO1187, ILE1192, TYR1224, GLY1185	O1 sp^3–Osp^3 SER1186: 3.261 O3 sp^3–Osp^2 HIS1201: 3.119 O2 sp^3–Osp^2 GLY1211: 3.167 O2 sp^3–Nsp^2 TYR1213: 3.049 O4 sp^3–Osp^2 PHE1214: 3.269	−67.28/0.52
Phloridzin	ILE1204, TYR1203, ILE1228, GLY1227, TYR1223, PRO1187, SER1186, SER1221, GLY1185, LYS1184, PHE1188, GLY1196, ALA1191, PHE1197, ASP1198, GLU1199, ARG1200, ALA1202, HIS1201, ALA1202, GLY1211, HIS1184	O9 sp^3–Osp^2 TYR1213: 2.977 O8 sp^3–Nsp^2 HIS1201: 2.688 O3 sp^3–Nsp^2 HIS1184: 2.752 O4 sp^3–Osp^2 HIS1201: 3.156 O2 sp^3–Osp^2 HIS1201: 3.002 O2 sp^3–Osp^2 ASP1198: 2.678	−74.58/0.82
Nothofagin	GLY1227, ILE1228, TYR1224, PRO1187, SER1186, GLY1185, GLU1291, SER1221, PHE1214, ALA1215, PHE1183, HIS1184, TYR1213, PHE1188, ALA1202, HIS1201, TYR1203, ARG1200, ILE1204, GLY1205	O2 sp^3–Nsp^2 HIS1201: 2.877 O5 sp^3–Osp^2 TYR1224: 3.085 O8 sp^2–Nsp^2 HIS1184: 3.026	−83.95/0.10
4-Methylchalcone	ILE1228, GLY1227, TYR1226, TYR1224, PRO1187, TYR1203, HIS1201, TYR1213, ALA1202, ILE1212, TYR1213, PHE1214, ALA1215, HIS1184, PHE1183, GLY1185, PHE1188, SER1186, LYS1220, TYR1224	No bonds	−67.80/0.12

The docking results reveal that the native ligand (the Co-crystallized 3J5A) had the greatest inhibitory score (−104.15) among the test ligands; this high score was due to the formation of four hydrogen bonds with three amino acid residues (GLU1291, SER1221, and GLY1185) in the TNKS1′ active pocket. Also, nothofagin presented the highest inhibitory score in the chalcones series (−84.47), followed by phloridzin (−74.58), chalcone (−69.30), 4-methylchalcone (−67.80), phloretin (−67.28) and benzophenone (−59.52). Benzophenone and 4-methylchalcone did not make hydrogen bridges with the amino acids in the active pocket; nevertheless, they show an inhibitory effect on TNKS1, most likely through hydrophobic bonds. Altogether, the docking scores suggest the ability of all six chalcone analogues to interfere with the activity of one important molecular target for carcinogenesis in humans, TNKS1, which is known to be responsible for the development and progression of colorectal cancer. Furthermore, the docking results emphasize the high inhibitory potential of the glycosylated derivatives in the series, as is also clear from the bioactivity computation studies (Table 2). Yet, glycosylated polyphenols do not usually

reach the inside of the (intestinal) cells in humans, as only their aglycones and metabolites do. Accordingly, the docking results must be seen in the context of molecular and quantum parameters and biophysical information, and also in the context of bioavailability data and formulation assemblage as well.

3.2. Pharmacological In Vitro Studies Results

In Vitro MTS Cytotoxicity and Anti-Proliferative Assessments

Pharmacological studies aimed to investigate the effects of three main chalcone derivatives in nature, phloretin (the aglycone form), phloridzin (the main *O*-glucoside found in the green plants) and 4-methylchalcone (the main chalcone metabolite in humans), upon the viability and the proliferation of the human tumor colon cells Caco-2 (ATCC, HTB-37). Studies were performed by the MTS method and cytotoxicity and anti-proliferative assays, respectively [46]. For the reference substance (r.s.) of the three test chalcones under investigation, each one was prepared as six dilution series, in 50% ethanol (*w*/*v*). The punctual concentrations obtained were as follows: 1, 5, 10, 25, 35, 50 µg test chalcone (r.s.) per 1 mL of sample. Tests were performed against negative control 1 (cells treated with Caco-2 growth medium only) and negative control 2 (cells treated with Caco-2 growth medium and 50% ethanol), in triplicate (n = 3). The use of two negative control series assures a better visualization of the effect of the solvent on the cells under investigation, and provides indications regarding the presence of some chemical species with protective effects against the potential harmful effects of alcohol on the environment. The results, O.D. at 492 nm and the percent (%) of cell viability along the dilution series were computed against negative control series 2, after which they were assigned for statistical signification; specifically, the notation (*) refers to results without statistical significance ($p > 0.05$); the notation (**) refers to results with statistical significance ($0.05 < p < 0.01$); and the notation (***) refers to results with high statistical significance ($p < 0.01$).

Figure 4a,b present the results on the in vitro MTS cytotoxicity assay after 24 h (h) of Caco-2 cell line exposure to the three chalcones under study, namely the phloretin/Phl, phloridzin/Phd and 4-metylchalcone/4MeCh dilution series, against the positive control series and the negative control series, with the mean values of the triplicates (n = 3), respectively.

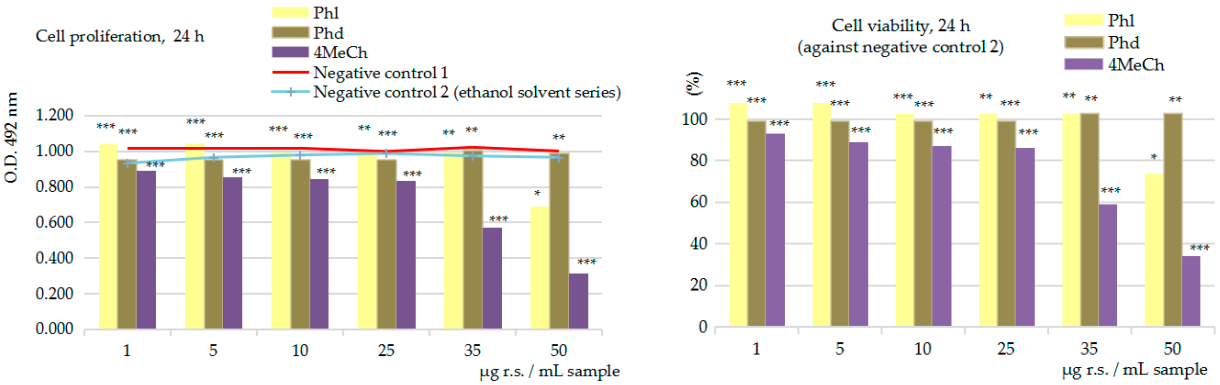

Figure 4. MTS cytotoxicity assay at 24 h after Caco-2 cell exposure to phloretin/Phl, phloridzin/Phd and 4-methylchalcone/4-MeCh at concentrations from 1 to 50 µg of test chalcone (r.s.) per sample: (**a**) The dynamic of the Caco-2 cell line proliferation and O.D. at 492 nm along the dilution series, in comparison with negative control series 2 (meaning Caco-2 cells treated with 50% ethanol—the blue line); the red line represents negative control series 1, meaning the Caco-2 cells in the presence of Caco-2 growth medium only; (**b**) the dynamic of the Caco-2 cell line viability and percents (%) along the dilution series, in comparison with negative control series 2. Where: notation * = results without statistical significance ($p > 0.05$); notation ** = results with statistical significance ($0.01 < p < 0.05$, $n = 3$, mean values); notation *** = results with statistical significance ($p < 0.01$, $n = 3$, mean values, relative to negative control series 2).

The analysis of the results in Figure 4, which compare the dynamic of the Caco-2 cell proliferation (a) and Caco-2 cell viability (b) along with the control positive series (the blue line) and the control negative series (the red line), specifically the results in the interval ranging from 1 to 35 µg of r.s. per sample, indicate the lack of cytotoxic effects in the case of phloretin and phloridzin; the 4-methylchalcone derivative indicated potential cytotoxic effects, starting with 1 µg of r.s. per sample. At the highest concentration in the study, 50 µg of r.s. per sample, both the 4-methylchacone derivate and the phloretin aglycone demonstrated cytotoxic effects. By comparison with the positive control series, the cell viability inhibitory effects were computed to be 66% in the case of 4-methylchalcone (4MeCh) and 26% in the case of phlorizin (Phl); phloridzin (Phd) did not affect the viability of the human tumor colon cells Caco-2 in vitro, not even at the highest concentration in the study (50 µg of r.s. per sample).

Figures 5a,b and 6a,b present the results of the in vitro MTS anti-proliferative assay after the 24 h and 48 h exposure of cells to the chalcone series, respectively; the results are the mean values of the test and positive/negative control series (n = 3).

Specifically, the MTS anti-proliferative assay on Caco-2 cells at 30% cell confluence indicated that, after 24 h of cell exposure (Figure 5), both 4-methylchalcone and phloretin aglycone induced a decrease in the proliferation (a) and the viability (b) of the human colon cancer cell line in vitro; their inhibitory effects started with 1 µg of r.s. per sample, and achieved 35% and 26% cell viability inhibition at the maximum concentration in the study (50 µg of r.s. per sample). Phloridzin emphasized the potential anti-proliferative effects upon the viability of the Caco-2 cell line at above 35 µg of r.s. per sample, and a maximum cell viability inhibition potential percentage ranging from 6 to 8% in the interval from 35 to 50 µg of r.s. per sample.

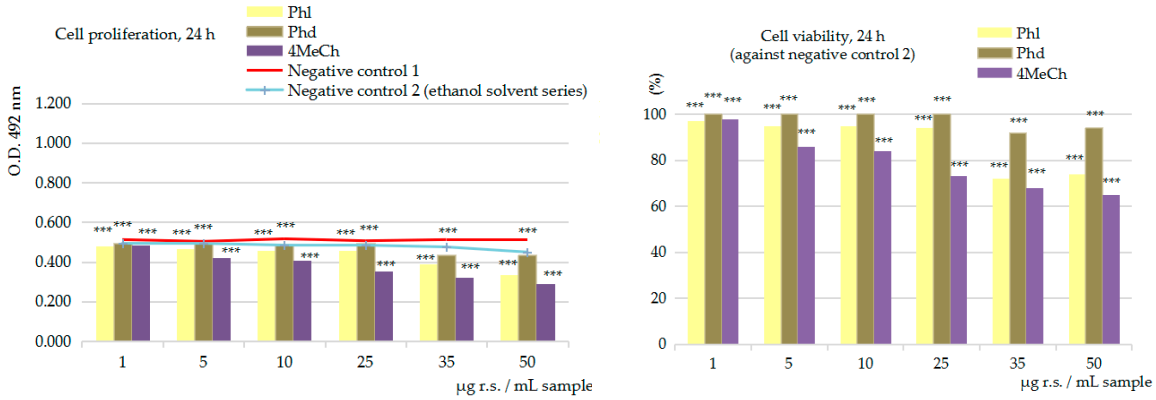

(**a**) (**b**)

Figure 5. MTS anti-proliferative assay at 24 h after Caco-2 cell exposure to phloretin/Phl, phloridzin/Phd and 4-methylchalcone/4-MeCh at concentrations from 1 to 50 µg of test chalcone (r.s.) per sample: (**a**) the dynamic of the Caco-2 cell line proliferation and O.D. at 492 nm along the dilution series, in comparison with negative control series 2 (meaning Caco-2 cells treated with 50% ethanol—the blue line); the red line represents negative control series 1, meaning the Caco-2 cells in the presence of Caco-2 growth medium only; (**b**) the dynamic of the Caco-2 cell line viability and percents (%) along the dilution series, in comparison with negative control series 2. Where: notation *** = results with statistical significance ($p < 0.01$, $n = 3$, mean values, relative to negative control series 2).

The MTS anti-proliferative assessment after 48 h of cell exposure to the three chalcone derivatives (Figure 6a,b), in comparison to the control positive (the blue line) and the control negative (the red line) series samples, both reconfirmed the ability of the 4-methylchalcone and phloretin derivatives to decrease the viability of the Caco-2 cells, with 1 µg of r.s. per sample. Specifically, phloretin (Phl) indicated a cell viability inhibition potential of up to 7% at 1 µg/mL sample, of up to 20% in the interval from 5 to 20 µg/mL, and of up to 34% in the interval from 35 to 50 µg/mL; 4-methylchalcone (4MeCh) has revealed a cell viability

inhibition potential of up to 10% in the interval from 1 to 25 µg/mL, and of up to 42% in the interval from 35 to 50 µg/mL; phloridzin's effects were computed at values ranging from −1% to +4% in the interval from 1 to 50 µg of r.s./sample; therefore, this study supports the lack of effect upon the Caco-2 cell viability in the cytotoxicity experiment.

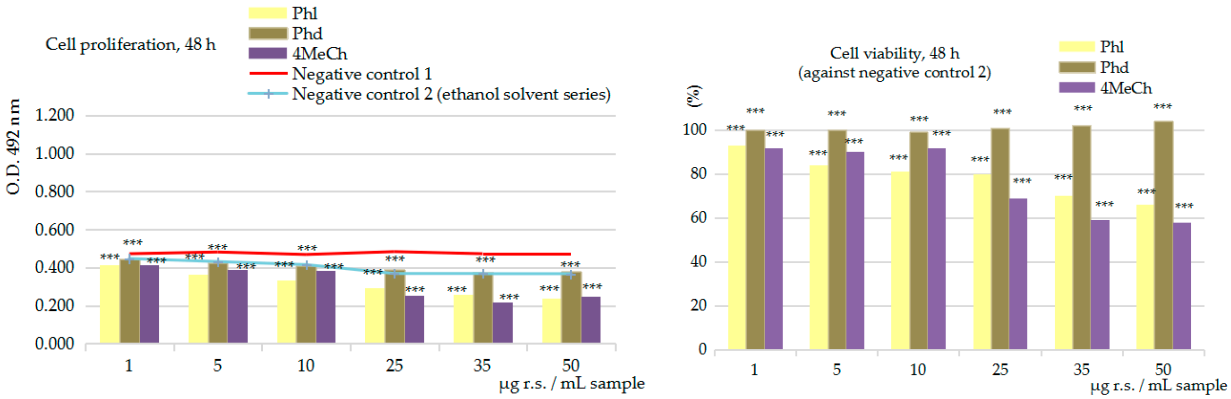

Figure 6. MTS anti-proliferative assay at 48 h after Caco-2 cell exposure to phloretin/Phl, phloridzin/Phd and 4-methylchalcone/4-MeCh at concentrations from 1 to 50 µg of test chalcone (r.s.) per sample: (**a**) the dynamic of the Caco-2 cell line proliferation and O.D. at 492 nm along the dilution series, in comparison with negative control series 2 (meaning Caco-2 cells treated with 50% ethanol—the blue line); the red line represents negative control series 1, meaning the Caco-2 cells in the presence of Caco-2 growth medium only; (**b**) the dynamic of the Caco-2 cell line viability and percent (%) along the dilution series, in comparison with negative control series 2. Where: notation *** = results with statistical significance ($p < 0.01$, $n = 3$, mean values, relative to negative control series 2).

4. Discussion

As is well known, symmetrical molecules are highly effective in targeting active proteins with symmetrical sub-unit arrangements or proteins that display a symmetrical arrangement of amino acids in their binding pockets. The planar lipophilic, and all the more planar lipophilic symmetrical molecules, are very effective pharmaceutical substances; at the same time, they have important side effects derived from their ability to switch the dipole moment of the cell membranes, causing chaotic effects or even the death of the cells. Diphenyl acetone derivatives and the top of the series, benzophenone, a symmetrical molecule, are the basis of countless biologically active compounds. On the other hand, the geometry, molecular size, and lipophilicity of biologically active molecules, are of primary interest in pharmaceutical chemistry and the global curative therapeutic market today. Diphenyl acetone derivatives, particularly chalcone analogues, are highly valued for their pharmacological activities and certain human health benefits. Analyzing these compounds through in silico and in vitro studies can provide valuable insights into their practical applications. As is known, information obtained through in silico computation is highly useful and practically necessary. The comparison of molecular, quantum, and bioactivity parameters across a series of chemical analogues can provide insights into their reactivity, bioavailability, and potential impact upon the function of the cells, leading to the prediction of the most appropriate formulation needs. Also, in silico docking studies targeting specific molecular sites can predict the effectiveness of the compounds in addressing key biological targets and pathologies.

Apart from the fact that they significantly reduce the time and the cost required to identify new active compounds for human health benefits, in silico studies can also be successfully utilized in the case of natural products, such as in food and dietary supplements, functional foods and cosmetics, which may not require or allow in vivo studies. These health products are usually recommended based on centuries of use for the treatment

of various health issues, while in silico computation may provide valuable data for their manufacturing and usage.

An example of the usefulness of bioactivity score computation in the food and dietary supplements industry is its ability to show the potential for some plant-derived products to act as broad enzyme inhibitors. Many plant-derived products are based on the total extracts, meaning that they contain most of the polyphenols found in the species. However, many polyphenolic compounds, especially flavonoid derivatives, are certain inhibitors of digestive enzymes in humans (e.g., amylase, protease, lipase, etc.). Products based on compounds with high inhibitory potency could negatively affect individuals with digestive enzyme disorders, making it essential to provide warnings or remedies about this possibility, e.g., the addition of digestive enzymes to drug formulations.

Another example of the usefulness of in silico studies in the field of natural medicines and plant-derived products is their ability to compute the lipophilicity and hydrophilicity character of key compounds. According to recent data, three of the top active anti-inflammatory compounds in green plants, namely curcumin, arctigenin and boswellic acid, require liposomal formulation to achieve their maximum bioavailability and effectiveness in humans [63–68]. This need could be predicted based on molecular parameters and by corroborating the log*P*, PSA, dipole moment, and HBA and HBD values.

Furthermore, chalcone derivatives are among the most active flavonoid subclasses found in green plants. Phloretin, the major chalcone aglycone in nature, can have potentially severe side effects on the cell function, but also acts as a highly effective anti-cancer remedy by providing chemopreventive, cytotoxic, antiproliferative, angiogenic and antimetastatic effects. In addition, according to in silico, in vitro and in vivo data, phloretin aglycone has the ability to cross the blood–brain barrier (log*P* = 2.05). These characteristics strongly recommend its use in neurological applications, for which there are only a few natural compounds available.

Supporting this, studies [69] have revealed the ability of phloretin aglycone to ameliorate 2-chlorohexadecanal-mediated brain microvascular cell disfunction in vitro; in fact, it completely abrogated 2-CIHDA-induced BMVEC barrier dysfunction and cell death. Studies have also proved the ability of phloretin to reduce the inflammatory phenotype of bone marrow-derived macrophages in vitro, as well as autoimmune encephalomyelitis neuroinflammation in a mice model; the effects were explained by phloretin's ability to induce autophagy-mediated Nrf2 (Nuclear factor erythroid 2-related factor 2) activation in macrophages [70].

Other combined studies, including in vitro (on macrophages), ex vivo (on cerebellar slice cultures) and in vivo (on mice model) approaches [71], have demonstrated that phloretin aglycone, at concentration levels ranging from 10 to 50 μM in vitro and ex vivo, and at 50 mg/kg body weight in vivo, can stimulate remyelination and thereby promote central nervous system (CNS) repair, specifically through the activation of the peroxizome proliferator-activated receptor gamma (PPARy) pathway. In vivo studies [72] on rats with chronic mild stress (CMS) induced by a variety of randomized stressors during a 3-week period also revealed phloretin's ability to decrease CMS-induced synapse losses by inhibiting the deposition of complement C3 onto synapsis and subsequent microglia-mediated synaptic engulfment; these findings suggest the potential of using phloretin chalcone in brain-targeted drug formulations.

Furthermore, introducing new active groups (e.g., hydroxyl, methyl, carboxyl, and alkene, heterocycles, etc.) and increasing the asymmetry of the molecule usually increase one or more pharmacological activities, as has been shown in the case of the anticancer activity of chalcone derivatives. Accordingly, it has been demonstrated that the introduction of new heterocyclic groups into the chalcone core can significantly enhance their anticancer activity [13,73–78]. These chalcone derivatives, with newly inserted N,S heterocyclic groups, can modulate a major pro-tumor sequence involving tubulin protein, the epidermal growth factor receptor (EGFR), and topoisomerase activity. Furthermore, the introduction of quinazoline and pyrazole groups into the chalcone core directly enhanced

their in vitro efficacy; in the specific case of the MCF-7 cell line, the new azole chalcones showed a decrease in IC_{50} values, below 0.01 μM; also, the incorporation of a piperazine moiety into the chalcone core resulted in the augmentation of multiple biological attributes, particularly increasing antioxidant, anti-inflammatory, anti-infective, and anticarcinogenic activities [73–76]. Finally, the introduction of some imidazole-type groups into the chalcone core led to increased cytotoxicity and a higher anti-proliferative potency [77,78].

Regarding the anticancer activity, studies conducted over time [11–15,79–97] have emphasized phloretin's ability to act against a wide range of human cancer cell lines in vitro; according to the data reported, their interval of efficacy ranged from 10 to 200 μM, with efficacy at concentrations greater than 50 μM. The reviewed studies [13–15] highlight phloretin aglycone's effectiveness against various cancers, including human oral cancer, human nasopharyngeal cancer, human esophageal cancer, human gastric cancer, colon cancer, human liver cancer, human cervical cancer, human ovarian cancer, human prostate cancer, human breast cancer, human lung cancer, human glioblastoma, human T-lymphocyte blood cancer, human leukemia, human erythroid leukemia and mouse melanoma cells. Similarly, apoptosis induction, the inhibition of cell migration and invasiveness, cell cycle arrest, and angiogenesis inhibition appear to be the most probable mechanisms of action in vitro [13–15], which converge to stimulate the apoptosis process via the intrinsic pathway.

The present study also aimed to investigate the effects of three main chalcone derivatives in nature, namely phloretin (the aglycone), phloridzin (the main *O*-glucoside derivate in green plants) and 4-methylchalcone (the main chalcone metabolite in humans), upon the viability of the human cancer colon line (Caco-2); the studies aimed to estimate their potential cytotoxic and antiproliferative effect at an interval of high interest for neurological and cancer applications, from 1 to 50 μg/mL, respectively. This way, the in vitro MTS cytotoxicity assay after 24 h of Caco-2 cell exposure to the three test chalcone dilution series indicated the cytotoxic potency of the 4-methylchalcone, against the no or slight effects of phloretin and phloridzin derivatives at 1 to 35 μg of reference substance (r.s.) per sample and between 35 and 50 μg of r.s. per sample for 4-methylchacone; phloretin aglycone also indicated potential cytotoxic effects (66% and 26% of cell viability inhibition, respectively), while phloridzin did not affect the viability of the Caco-2 cells. Subsequently, MTS anti-proliferative studies at 24 h and 48 h practically refined the cytotoxic potency of the three chalcone derivates under study. Accordingly, after 24 h of young Caco-2 cell culture exposure to the three test chalcones, it was observed that 4-methylchalcone and phloretin started to decrease the viability of the Caco-2 cells with 1 μg of r.s. per sample, while phloridzin decreased the viability with 35 μg of r.s. per sample; at the maximum concentration in the study, 50 μg of r.s. per sample, 4-methylchacone and phloretin achieved up to 35% and 26% cell viability inhibition, respectively. Phloridzin indicated up to 8% cell viability inhibition. After 48 h of Caco-2 cell exposure, the results were as follows: phloretin achieved up to 7% inhibitory potency at 1 μg per sample, up to 20% in the interval from 5 to 20 μg per sample and up to 34% in the interval from 35 to 50 μg per sample; 4-methylchalcone achieved a cell viability inhibition efficacy up to 10% in the interval from 1 to 25 μg per sample and up to 42% in the interval from 35 to 50 μg per sample; and phloridzin indicated no effects on the Caco-2 cell viability in the interval from 1 to 50 μg per sample. Therefore, the conclusion drawn in the cytotoxicity assay was confirmed, with there being a lack of activity upon the Caco-2 cells, respectively.

Regarding the ability of in silico studies to estimate the behavior of the compounds in vitro, the bioactivity scores in the present study suggest a high bioactivity score for phloretin and phloridzin versus a decreased bioactivity score for 4-methylchalcone; in addition, the docking studies against one suggestive molecular target for colon cancer development in humans, the TNKS1 enzyme, indicated the following scale of inhibitory potency along the chalcone' analogues: phloridzin > 4-methylchalcone > phloretin. In practice, in vitro studies on human cancer colon cell line Caco-2 have demonstrated the lack of activity of phloridzin, in both cytotoxicity and anti-proliferative assays, while phloretin

presents activity over 35 μg of r.s. per sample in the cytotoxicity assay, and starting with 1 μg of r.s. per sample in the anti-proliferative assay; in contrast, the 4-methylchalcone derivate showed broad activity in both in vitro assays, along the entire interval tested (1–50 μg r.s. per sample). These apparently inconsistent results could also be explained by taking into account the bioavailability predictions (log*P*) for the three tested compounds, which in fact suggested the ability of 4-methylchalcone and phloretin to cross the intestinal cell barrier (log*P* = 4.25 and log*P* = 2.05), compared to the low bioavailability of the phloridzin derivate (log*P* = 0.21) in humans, likely explaining its inefficacy in vitro.

5. Conclusions

The diphenyl acetone-type structure, specifically the chalcone core, is at the basis of the most used active series in green plants, the polyphenol class; therefore, chalcone derivatives are of increased interest for health industries today. At the same time, in silico studies can be successfully used for the prediction of numerous chemical, biophysical and pharmacological attributes of natural and synthetic biologically active molecules.

In the current study, by in silico and in vitro investigations of six chalcone analogues (benzophenone, chalcone, phloretin, nothofagin, phloridzin and 4-methylchalcone) of high chemical pharmaceutical interest, valuable information regarding their practical usefulness and potential negative effects upon humans was obtained.

In this way, in silico studies of the molecular, quantum and bioactivity parameters of the six chalcone analogues under study showed the ability of phloretin aglycone to cross the blood–brain barrier, as well as phloridzin and nothofagin's potential to interfere with the activity of the digestive enzymes in humans. The in vitro MTS studies on phloretin (the main chalcone aglycone in nature), phloridzin (the main chalcone-*O*-glucoside derivate in green plants) and 4-methylchalcone (the main chalcone metabolite in humans), tested for their effects on the viability of the Caco-2 cell line, showed that phloretin and 4-methylchalcone induced both cytotoxic and antiproliferative effects on the human cancer colon cells, whereas phloridzin did not influence the viability of the Caco-2 cell line in vitro. Specifically, phloretin and 4-methylchalcone induced anti-proliferative effects along the entire interval from 1 to 50 μg of r.s. per sample; the cytotoxic effects were noticed at 50 μg of r.s. per sample in the case of phloretin and started with 1 μg of r.s. per sample in the case of the 4-methy derivative.

These results show that phloretin, in equivalent doses under 35 μg per sample in vitro, may have protective anti-tumor effects on human intestinal cells.

Supplementary Materials: The following supporting information can be downloaded at: https://www.mdpi.com/article/10.3390/sym16101383/s1, Figure S1: Repartition of the frontier molecular orbitals (HOMO and LUMO) and their energy level diagrams for the six test compounds under study; Figure S2: Atom labeling and pose docking pose with or without hydrogen bonding within the active site of TNKS1 for the six test compounds under study.

Author Contributions: Conceptualization, L.C.P.; methodology, G.N. and A.S.; software, A.S.; validation, L.C.P., G.N. and A.S.; formal analysis, G.N. and A.A.; investigation, G.N., A.A. and A.S.; resources, A.S. and L.C.P.; data curation, L.C.P. and N.R.; writing—original draft preparation, L.C.P.; writing—review and editing, L.C.P. and A.S.; visualization L.C.P.; supervision, L.C.P.; project administration, L.C.P.; funding acquisition, L.C.P. All authors have read and agreed to the published version of the manuscript.

Funding: This research was funded by "Nucleu" Program, UEFISCDI, Grant no. 1N/2023, Project code PN23–28 BioChemLife" within the National Plan for Research Development and Innovation 2022–2027, carried out with the support of MCID and belong to the project PN 23-28 04 01.

Data Availability Statement: The original contributions presented in the study are included in the article/Supplementary Material; further inquiries can be directed to the corresponding author. The raw data from computations supporting the conclusions of this article will be made available by the authors upon request.

Conflicts of Interest: The authors declare no conflicts of interest.

References

1. Efimova, S.S.; Ostroumova, O.S. Effect of dipole modifiers on the magnitude of the dipole potential of sterol-containing bilayers. *Langmuir* **2012**, *28*, 9908–9914. [CrossRef]
2. Stewart, M.P.; Langer, R.; Jensen, K.F. Intracellular Delivery by Membrane Disruption: Mechanisms, Strategies, and Concepts. *Chem. Rev.* **2018**, *118*, 7409–7531. [CrossRef]
3. Cseh, R.; Benz, R. Interaction of phloretin with lipid monolayers: Relationship between structural changes and dipole potential change. *Biophys. J.* **1999**, *77*, 1477–1488. [CrossRef]
4. Sukhorukov, V.L.; Kürschner, M.; Dilsky, S.; Lisec, T.; Wagner, B.; Schenk, W.A.; Benz, R.; Zimmermann, U. Phloretin-induced changes of lipophilic ion transport across the plasma membrane of mammalian cells. *Biophys. J.* **2001**, *81*, 1006–1013. [CrossRef]
5. Sanmartin, C.; Font, M.; Palop, J.A. Molecular symmetry: A structural property frequently present in new cytotoxic and proapoptotic drugs. *Mini Rev. Med. Chem.* **2006**, *6*, 639–650. [CrossRef]
6. Rosini, E.; Pollegioni, L.; Molla, G. The Symmetric Active Site of Enantiospecific Enzymes. *Symmetry* **2023**, *15*, 1017. [CrossRef]
7. Chrusciel, P.; Goodford, P.J. Symmetry in drug molecules (proceedings). *Br. J. Pharmacol.* **1979**, *66*, 80P. [PubMed] [PubMed Central]
8. Surana, K.; Chaudhary, B.; Diwaker, M.; Sharma, S. Benzophenone: A ubiquitous scaffold in medicinal chemistry. *MedChemComm* **2018**, *9*, 1803–1817. [CrossRef]
9. Neveu, V.; Perez-Jiménez, J.; Vos, F.; Crespy, V.; du Chaffaut, L.; Mennen, L.; Knox, C.; Eisner, R.; Cruz, J.; Wishart, D.; et al. Phenol-Explorer: An online comprehensive database on polyphenol contents in foods. *Database* **2010**, *2010*, bap024. [CrossRef]
10. Niederberge, K.E.; Tennant, D.R.; Bellion, P. Dietary intake of phloridzin from natural occurrence in foods. *Br. J. Nutr.* **2020**, *123*, 942–950. [CrossRef]
11. Orlikova, B.; Tasdemir, D.; Golais, F.; Dicato, M.; Diederich, M. Dietary chalcones with chemopreventive and chemotherapeutic potential. *Genes Nutr.* **2011**, *6*, 125–147. [CrossRef]
12. De Matos, M.J.; Vazquez-Rodriguez, S.; Uriarte, E.; Santana, L. Potential pharmacological uses of chalcones: A patent review. *Expert. Opin. Ther. Pat.* **2015**, *25*, 351–366.
13. Salehi, B.; Quispe, C.; Chamkhi, I.; El Omari, N.; Balahbib, A.; Sharifi-Rad, J.; Bouyahya, A.; Akram, M.; Iqbal, M.; Docea, A.O.; et al. Pharmacological Properties of Chalcones: A Review of Preclinical Including Molecular Mechanisms and Clinical Evidence. *Front. Pharmacol.* **2021**, *11*, 592654. [CrossRef]
14. Tuli, H.S.; Rath, P.; Chauhan, A.; Ramniwas, S.; Vashishth, K.; Varol, M.; Jaswal, V.S.; Haque, S.; Sak, K. Phloretin, as a Potent Anticancer Compound: From Chemistry to Cellular Interactions. *Molecules* **2022**, *27*, 8819. [CrossRef]
15. Kartik, T.N.; Hemant, B.; Rajesh, C.; Kalyani, S.; Yogeeta, O.A.; Charu, S.; Shreesh, O.; Sameer, N.G. Therapeutic Potential and Pharmaceutical Development of a Multitargeted Flavonoid Phloretin. *Nutrients* **2022**, *14*, 3638. [CrossRef]
16. Baell, J.B. Feeling Nature's PAINS: Natural Products, Natural Product Drugs, and Pan Assay Interference Compounds (PAINS). *J. Nat. Prod.* **2016**, *79*, 616–628. [CrossRef]
17. De Matos, A.M.; Blázquez-Sánchez, M.T.; Sousa, C.; Oliveira, M.C.; De Almeida, R.F.M.; Rauter, A.P. C-Glucosylation as a tool for the prevention of PAINS-induced membrane dipole potential alterations. *Sci. Rep.* **2021**, *11*, 4443. [CrossRef]
18. Londzin, P.; Siudak, S.; Cegieła, U.; Pytlik, M.; Janas, A.; Waligóra, A.; Folwarczna, J. Phloridzin, an Apple Polyphenol, Exerted Unfavorable Effects on Bone and Muscle in an Experimental Model of Type 2 Diabetes in Rats. *Nutrients* **2018**, *10*, 1701. [CrossRef]
19. Zhao, Y.Y.; Fan, Y.; Wang, M.; Wang, J.; Cheng, J.X.; Zou, J.B.; Zhang, X.F.; Shi, Y.J.; Guo, D.Y. Studies on pharmacokinetic properties and absorption mechanism of phloretin: In vivo and in vitro. *Biomed. Pharmacother.* **2020**, *132*, 110809. [CrossRef]
20. Behzad, S.; Sureda, A.; Barreca, D.; Nabavi, S.F.; Rastrelli, L.; Nabavi, S.M. Health effects of phloretin: From chemistry to medicine. *Phytochem. Rev.* **2017**, *16*, 527–533. [CrossRef]
21. Remsberg, C.M.; Yáñez, J.A.; Vega-Villa, K.; Miranda, N.D.; Andrews, P.K. HPLC-UV Analysis of Phloretin in Biological Fluids and Application to Pre-Clinical Pharmacokinetic Studies. *J. Chromatogr. Sep. Technol.* **2010**, *1*, 101. [CrossRef]
22. Abu-Azzam, O.; Nasr, M. In vitro anti-inflammatory potential of phloretin microemulsion as a new formulation for prospective treatment of vaginitis. *Pharm. Dev. Technol.* **2020**, *25*, 930–935. [CrossRef]
23. Guo, D.; Liu, J.; Fan, Y.; Cheng, J.; Shi, Y.; Zou, J.; Zhang, X. Optimization, characterization and evaluation of liposomes from *Malus hupehensis* (Pamp.) Rehd. extracts. *J. Liposome Res.* **2020**, *30*, 366–376. [CrossRef]
24. Karabulut, S.; Toprak, M. Biophysical study of phloretin with human serum albumin in liposomes using spectroscopic methods. *Eur. Biophys. J.* **2020**, *49*, 463–472. [CrossRef]
25. Wang, Y.; Li, D.; Lin, H.; Jiang, S.; Han, L.; Hou, S.; Lin, S.; Cheng, Z.; Bian, W.; Zhang, X.; et al. Enhanced oral bioavailability and bioefficacy of phloretin using mixed polymeric modified self-nanoemulsions. *Food Sci. Nutr.* **2020**, *8*, 3545–3558. [CrossRef]
26. Sinha, S.; Prakash, A.; Medhi, B.; Sehgal, A.; Batovska, D.I.; Sehgal, R. Pharmacokinetic evaluation of Chalcone derivatives with antimalarial activity in New Zealand White Rabbits. *BMC Res. Notes* **2021**, *14*, 264. [CrossRef]
27. Pandey, R.P.; Li, T.F.; Kim, E.-H.; Yamaguchi, T.; Park, Y.I.; Kim, J.S.; Sohng, J.K. Enzymatic Synthesis of Novel Phloretin Glucosides. *Appl. Environ. Microbiol.* **2013**, *79*, 3516–3521. [CrossRef]
28. Wang, L.; Li, Z.W.; Zhang, W.; Xu, R.; Gao, F.; Liu, Y.F.; Li, Y.J. Synthesis, Crystal Structure, and Biological Evaluation of a Series of Phloretin Derivatives. *Molecules* **2014**, *19*, 16447–16457. [CrossRef]
29. Higgs, J.; Wasowski, C.; Marcos, A.; Jukič, M.; Paván, C.; Gobec, S.; de Tezanos Pinto, F.; Colettis, N.; Marder, M. Chalcone derivatives: Synthesis, in vitro and in vivo evaluation of their anti-anxiety, anti-depression and analgesic effects. *Heliyon* **2019**, *5*, e01376. [CrossRef]

30. Minsat, L.; Peyrot, C.; Brunissen, F.; Renault, J.-H.; Allais, F. Synthesis of Biobased Phloretin Analogues: An Access to Antioxidant and Anti-Tyrosinase Compounds for Cosmetic Applications. *Antioxidants* **2021**, *10*, 512. [CrossRef]
31. Peerce, B.E.; Clarke, R. A phosphorylated phloretin derivative. Synthesis and effect on intestinal Na(+)-dependent phosphate absorption. *Am. J. Physiol. Liver Physiol.* **2022**, *0641*, 848–855.
32. Halgren, T.A. Merck molecular force field. I. Basis, form, scope, parameterization, and performance of MMFF94. *J. Comput. Chem.* **1996**, *17*, 490–519. [CrossRef]
33. Shao, Y.; Molnar, L.F.; Jung, Y.; Kussmann, J.; Ochsenfeld, C.; Brown, S.T.; Gilbert, A.T.B.; Slipchenko, L.V.; Levchenko, S.V.; O'Neill, D.P.; et al. Advances in methods and algorithms in a modern quantum chemistry program package. *Phys. Chem. Chem. Phys.* **2006**, *8*, 3172–3191. [CrossRef]
34. Parr, R.G.; Yang, W. *Density Functional Theory of Atoms and Molecules*; Oxford University Press: Oxford, UK, 1989; Volume 16.
35. Lee, C.; Yang, W.; Parr, R.G. Development of the Colle-Salvetti correlation-energy formula into a functional of the electron density. *Phys. Rev. B* **1988**, *37*, 785–789. [CrossRef]
36. Hehre, W.J. *A Guide to Molecular Mechanics and Quantum Chemical Calculations*; Wavefunction, Inc.: Irvine, CA, USA, 2003; pp. 6–311.
37. Ciocirlan, O.; Ungureanu, E.-M.; Vasile (Corbei), A.-A.; Stefaniu, A. Properties Assessment by Quantum Mechanical Calculations for Azulenes Substituted with Thiophen– or Furan–Vinyl–Pyridine. *Symmetry* **2022**, *14*, 354. [CrossRef]
38. Vasile (Corbei), A.-A.; Ungureanu, E.-M.; Stanciu, G.; Cristea, M.; Stefaniu, A. Evaluation of (Z)-5-(Azulen-1-ylmethylene)-2-thioxothiazolidin-4-ones Properties Using Quantum Mechanical Calculations. *Symmetry* **2021**, *13*, 1462. [CrossRef]
39. Stefaniu, A.; Pirvu, L. In silico study approach upon a series of 50 polyphenolic compounds in plants; a comparison on the bioavailability and bioactivity data. *Molecules* **2022**, *27*, 1413. [CrossRef]
40. Molinspiration Cheminformatics Free Web Services. Slovensky Grob, Slovakia. Available online: https://www.molinspiration.com (accessed on 16 July 2024).
41. Pinto, D.; Gregorieff, A.; Begthel, H.; Clevers, H. Canonical Wnt signals are essential for homeostasis of the intestinal epithelium. *Genes Dev.* **2003**, *17*, 1709–1713. [CrossRef]
42. He, K.; Gan, W.J. Wnt/β-Catenin Signaling Pathway in the Development and Progression of Colorectal Cancer. *Cancer Manag. Res.* **2023**, *15*, 435–448. [CrossRef]
43. Johannes, J.W.; Almeida, L.; Barlaam, B.; Boriack-Sjodin, P.A.; Casella, R.; Croft, R.A.; Dishington, A.P.; Gingipalli, L.; Gu, C.; Hawkins, J.L.; et al. Pyrimidinone Nicotinamide Mimetics as Selective Tankyrase and Wnt Pathway Inhibitors Suitable for in Vivo Pharmacology. *ACS Med. Chem. Lett.* **2015**, *6*, 254–259. [CrossRef]
44. Neagu, G.; Stefaniu, A.; Albulescu, A.; Pintilie, L.; Pirvu, L. Antiproliferative activity of Stokesia laevis ethanolic extract in combination with several food-related bioactive compounds; in vitro (Caco2) and in silico docking (TNKS1 and TNKS2) studies. *Appl. Sci.* **2021**, *11*, 9944. [CrossRef]
45. Pirvu, L.; Stefaniu, A.; Neagu, G.; Pintilie, L. Studies on Anemone nemorosa L. extracts; polyphenols profile, antioxidant activity, and effects on Caco-2 cells by in vitro and in silico studies. *Open Chem.* **2022**, *20*, 299–312. [CrossRef]
46. Protocols & Applications Guide. Available online: https://www.promega.com (accessed on 20 September 2023).
47. Ghose, A.K.; Pritchett, A.; Crippen, G.M. Atomic physicochemical parameters for three dimensional structure directed quantitative structure-activity relationships III: Modeling hydrophobic interactions. *J. Comput. Chem.* **1988**, *9*, 80–90. [CrossRef]
48. Leo, A.; Hansch, C.; Elkins, D. Partition Coefficients and their uses. *Chem. Rev.* **1971**, *6*, 525–616. [CrossRef]
49. Greenberg, M.J. The importance of hydrophobic properties of organic compounds on their taste intensities: A quantitative structure-taste-intensity study. *J. Agric. Food Chem.* **1980**, *28*, 562–566. [CrossRef]
50. Hansch, C.; Björkrot, J.B.; Leo, A. Hydrophobicity and Central Nervous System Agents: On the Principle of Minimal Hydrophobicity in Drug Design. *J. Pharm. Sci.* **1987**, *76*, 663–687. [CrossRef]
51. Ruiz, P.; Begluitti, G.; Tincher, T.; Wheeler, J.; Mumtaz, M. Prediction of Acute Mammalian Toxicity Using QSAR Methods: A Case Study of Sulfur Mustard and Its Breakdown Products. *Molecules* **2012**, *17*, 8982–9001. [CrossRef]
52. Bhal, S.K. *LogP—Making Sense of the Value*; Advanced Chemistry Development, Inc.: Toronto, ON, Canada, 2007. Available online: https://www.acdlabs.com/wp-content/uploads/download/app/physchem/making_sense.pdf (accessed on 14 August 2024).
53. Vo, M.N.; Call, M.; Kowall, C.; Johnson, J.K. Method for Predicting Dipole Moments of Complex Molecules for Use in Thermophysical Property Estimation. *Ind. Eng. Chem. Res.* **2019**, *58*, 19263–19270. [CrossRef]
54. Avramopoulos, A.; Reis, H.; Li, J.; Papadopoulos, M.G. The dipole moment, polarizabilities, and first hyperpolarizabilities of HArF. A computational and comparative study. *J. Am. Chem. Soc.* **2004**, *126*, 6179–6184. [CrossRef]
55. Zhou, D.; Porter, W.R.; Zhang, G.G.Z. Chapter 5—Drug Stability and Degradation Studies. In *Developing Solid Oral Dosage Forms Pharmaceutical Theory and Practice*, 2nd ed.; Qiu, Y., Chen, Y., Zhang, G., Yu, L., Mantri, R.V., Eds.; Academic Press: Cambridge, MA, USA, 2016; pp. 113–149.
56. Lipinski, C.A.; Lombardo, F.; Dominy, B.W.; Feeney, P.J. Experimental and computational aproaches to estimate solubility and permeability in drug discovery and development settings. *Adv. Drug Deliv. Rev.* **2001**, *46*, 3–26. [CrossRef]
57. Flores-Holguín, N.; Frau, J.; Glossman-Mitnik, D. Chemical Reactivity Properties and Bioactivity Scores of the Angiotensin II Vasoconstrictor Octapeptide. In *Cheminformatics and Its Applications*; Stefaniu, A., Rasul, A., Hussain, G., Eds.; IntechOpen: London, UK, 2020; pp. 78–79; ISBN 978-1-83880-068-0.

58. Khan, T.; Dixit, S.; Ahmad, R.; Raza, S.; Azad, I.; Joshi, S.; Khan, A.R. Molecular docking, PASS analysis, bioactivity score prediction, synthesis, characterization and biological activity evaluation of a functionalized 2-butanone thiosemicarbazone ligand and its complexes. *J. Chem. Biol.* **2017**, *10*, 91–104. [CrossRef]
59. Sastri, V.S.; Perumareddi, J.R. Molecular orbital theoretical studies of some organic corrosion inhibitors. *Corros. Sci.* **1997**, *53*, 617–622. [CrossRef]
60. Yankova, R.; Genieva, S.; Halachev, N.; Dimitrova, G. Molecular structure, vibrational spectra, MEP, HOMO-LUMO and NBO analysis of $Hf(SeO_3)(SeO_4)(H_2O)_4$. *J. Mol. Struct.* **2016**, *1106*, 82–88. [CrossRef]
61. Yılmaza, M.; Kebiroğlub, M.H. Structural Changes in 2-Acetoxybenzoic Acid (2ABA) in the Presence of Various Solvents: A Quantum Chemical and Spectroscopic Study. *J. Phys. Chem. Funct. Mater.* **2024**, *7*, 38–46. [CrossRef]
62. Forman, H.J.; Davies, K.J.; Ursini, F. How do nutritional antioxidants really work: Nucleophilic tone and para-hormesis versus free radical scavenging in vivo. *Free Radic. Biol. Med.* **2014**, *66*, 24–35. [CrossRef]
63. Prasad, S.; Tyagi, A.K.; Aggarwal, B.B. Recent developments in delivery, bioavailability, absorption and metabolism of curcumin: The golden pigment from golden spice. *Cancer Res. Treat.* **2014**, *46*, 2–18. [CrossRef]
64. Abd El-Hack, M.E.; El-Saadony, M.T.; Swelum, A.A.; Arif, M.; Abo Ghanima, M.M.; Shukry, M.; Noreldin, A.; Taha, A.E.; El-Tarabily, K.A. Curcumin, the active substance of turmeric: Its effects on health and ways to improve its bioavailability. *J. Sci. Food Agric.* **2021**, *101*, 5747–5762. [CrossRef]
65. Li, J.; Li, X.; Ren, Y.-S.; Lv, Y.-Y.; Zhang, J.-S.; Xu, X.-L.; Wang, X.-Z.; Yao, J.-C.; Zhang, G.-M.; Liu, Z. Elucidation of Arctigenin Pharmacokinetics and Tissue Distribution after Intravenous, Oral, Hypodermic and Sublingual Administration in Rats and Beagle Dogs: Integration of In Vitro and In Vivo Findings. *Front. Pharmacol.* **2017**, *8*, 376. [CrossRef]
66. Liu, S.; He, Y.; Feng, M.; Huang, Y.; Wu, W.; Wang, J. Targeted Delivery of Arctigenin Using Sialic Acid Conjugate-Modified Liposomes for the Treatment of Breast Cancer. *Molecules* **2024**, *29*, 278. [CrossRef]
67. Sharma, A.; Gupta, N.K.; Dixit, V.K. Complexation with phosphatidyl choline as a strategy for absorption enhancement of boswellic acid. *Drug Deliv.* **2010**, *17*, 587–595. [CrossRef]
68. Mehta, M.; Dureja, H.; Garg, M. Development and optimization of boswellic acid-loaded proniosomal gel. *Drug Deliv.* **2016**, *23*, 3072–3081. [CrossRef]
69. Ullen, A.; Fauler, G.; Bernhart, E.; Nusshold, C.; Reicher, H.; Leis, H.J.; Malle, E.; Sattler, W. Phloretin ameliorates 2-chlorohexadecanal-mediated brain microvascular endothelial cell dysfunction in vitro. *Free Radic. Biol. Med.* **2012**, *53*, 1770–1781. [CrossRef]
70. Dierckx, T.; Haidar, M.; Grajchen, E.; Wouters, E.; Vanherle, S.; Loix, M.; Boeykens, A.; Bylemans, D.; Hardonnière, K.; Kerdine-Römer, S.; et al. Phloretin suppresses neuroinflammation by autophagy-mediated Nrf2 activation in macrophages. *J. Neuroinflamm.* **2021**, *18*, 148. [CrossRef]
71. Dierckx, T.; Vanherle, S.; Haidar, M.; Grajchen, E.; Mingneau, F.; Gervois, P.; Wolfs, E.; Bylemans, D.; Voet, A.; Nguyen, T.; et al. Phloretin enhances remyelination by stimulating oligodendrocyte precursor cell differentiation. PNAS. *Neuroscience* **2022**, *119*, e2120393119. [CrossRef]
72. Li, C.; Liu, B.; Xu, J.; Jing, B.; Guo, L.; Wang, L.; Wang, M.; Zhang, H.; He, Q.; Yu, X.; et al. Phloretin decreases microglia-mediated synaptic engulfment to prevent chronic mild stress-induced depression-like behaviors in the mPFC. *Theranostics* **2023**, *13*, 955–972. [CrossRef]
73. Sheikh, K.A.; Gupta, A.; Umar, M.; Ali, R.; Shaquiquzzaman, M.; Akhter, M.; Khan, M.A.; Kaleem, M.; Ambast, P.K.; Charan, S.; et al. Advances in chalcone derivatives: Unravelling their anticancer potential through structure-activity studies. *J. Mol. Struct.* **2024**, *1299*, 137154. [CrossRef]
74. Sharma, V.; Kumar, V.; Kumar, P. Heterocyclic chalcone analogues as potential anticancer agents. *Anticancer Agents Med. Chem.* **2013**, *13*, 422–432.
75. Yang, J.; Lv, J.; Cheng, S.; Jing, T.; Meng, T.; Huo, D.; Ma, X.; Wen, R. Recent Progresses in Chalcone Derivatives as Potential Anticancer Agents. *Anticancer Agents Med. Chem.* **2023**, *23*, 1265–1283. [CrossRef]
76. Shukla, S.; Sood, A.K.; Goyal, K.; Singh, A.; Sharma, V.; Guliya, N.; Gulati, S.; Kumar, S. Chalcone Scaffolds as Anticancer Drugs: A Review on Molecular Insight in Action of Mechanisms and Anticancer Properties. *Anticancer Agents Med. Chem.* **2021**, *21*, 1650–1670. [CrossRef]
77. Djemoui, A.; Naouri, A.; Ouahrani, M.R.; Djemoui, D.; Lahcene, S.; Lahrach, M.B.; Boukenna, L.; Albuquerque, H.; Saher, L.; Rocha, D.H.A.; et al. A step-by-step synthesis of triazole-benzimidazole-chalcone hybrids: Anticancer activity in human cells. *J. Mol. Struct.* **2020**, *1204*, 127487. [CrossRef]
78. Oskuei, R.S.; Mirzaei, S.; Jafari-Nik, M.R.; Hadizadeh, F.; Eisvand, F.; Mosaffa, F.; Ghodsi, R. Design, synthesis and biological evaluation of novel imidazole-chalcone derivatives as potential anticancer agents and tubulin polymerization inhibitors. *Bioorg. Chem.* **2021**, *112*, 104904. [CrossRef]
79. Kobori, M.; Iwashita, K.; Shinmoto, H.; Tsushida, T. Phloretin-induced apoptosis in B16 melanoma 4A5 cells and HL60 human leukemia cells. *Biosci. Biotechnol. Biochem.* **1999**, *63*, 719–725. [CrossRef]
80. Kim, M.S.; Kwon, J.Y.; Kang, N.J.; Lee, K.W.; Lee, H.J. Phloretin induces apoptosis in H-Ras MCF10A human breast tumor cells through the activation of p53 via JNK and p38 mitogen-activated protein kinase signaling. *Ann. N. Y. Acad. Sci.* **2009**, *1171*, 479–483. [CrossRef]

81. Wu, C.H.; Ho, Y.S.; Tsai, C.Y.; Wang, Y.J.; Tseng, H.; Wei, P.L.; Lee, C.H.; Liu, R.S.; Lin, S.Y. In vitro and in vivo study of phloretin-induced apoptosis in human liver cancer cells involving inhibition of type II glucose transporter. *Int. J. Cancer* **2009**, *124*, 2210–2219. [CrossRef]
82. Lu, M.; Kong, Q.; Xu, X.; Lu, H.; Lu, Z.; Yu, W.; Zuo, B.; Su, J.; Guo, R. Evaluation of apoptotic and growth inhibitory activity of phloretin in BGC823 gastric cancer cell. *Trop. J. Pharm. Res.* **2015**, *14*, 27–31. [CrossRef]
83. Min, J.; Li, X.; Huang, K.; Tang, H.; Ding, X.; Qi, C.; Qin, X.; Xu, Z. Phloretin induces apoptosis of non-small cell lung carcinoma A549 cells via JNK1/2 and p38 MAPK pathways. *Oncol. Rep.* **2015**, *34*, 871–2879. [CrossRef]
84. Duan, H.; Wang, R.; Yan, X.; Liu, H.; Zhang, Y.; Mu, D.; Han, J.; Li, X. Phloretin induces apoptosis of human esophageal cancer via a mitochondria-dependent pathway. *Oncol. Lett.* **2017**, *14*, 6763. [CrossRef]
85. Zhou, M.; Zheng, J.; Bi, J.; Wu, X.; Lyu, J.; Gao, K. Synergistic inhibition of colon cancer cell growth by a combination of atorvastatin and phloretin. *Oncol. Lett.* **2018**, *15*, 1985–1992. [CrossRef]
86. Wu, K.H.; Ho, C.T.; Chen, Z.F.; Chen, L.C.; Whang-Peng, J.; Lin, T.N.; Ho, Y.S. The apple polyphenol phloretin inhibits breast cancer cell migration and proliferation via inhibition of signals by type 2 glucose transporter. *J. Food Drug Anal.* **2018**, *26*, 221–231. [CrossRef]
87. Geohagen, B.C.; Korsharskyy, B.; Vydyanatha, A.; Nordstroem, L.; LoPachin, R.M. Phloretin cytoprotection and toxicity. *Chem. Biol. Interact.* **2018**, *296*, 117–123. [CrossRef]
88. Hsiao, Y.H.; Hsieh, M.J.; Yang, S.F.; Chen, S.P.; Tsai, W.C.; Chen, P.N. Phloretin suppresses metastasis by targeting protease and inhibits cancer stemness and angiogenesis in human cervical cancer cells. *Phytomedicine* **2019**, *62*, 152964. [CrossRef]
89. Saraswati, S.; Alhaider, A.; Abdelgadir, A.M.; Tanwer, P.; Korashy, H.M. Phloretin attenuates STAT-3 activity and overcomes sorafenib resistance targeting SHP-1-mediated inhibition of STAT3 and Akt/VEGFR2 pathway in hepatocellular carcinoma. *Cell Commun. Signal.* **2019**, *17*, 127. [CrossRef]
90. Choi, B.Y. Biochemical Basis of Anti-Cancer-Effects of Phloretin—A Natural Dihydrochalcone. *Molecules* **2019**, *24*, 278. [CrossRef]
91. Jin, G.; Zhao, Z.; Chakraborty, T.; Mandal, A.; Roy, A.; Roy, S.; Guo, Z. Decrypting the Molecular Mechanistic Pathways Delineating the Chemotherapeutic Potential of Ruthenium-Phloretin Complex in Colon Carcinoma Correlated with the Oxidative Status and Increased Apoptotic Events. *Oxid. Med. Cell. Longev.* **2020**, *2020*, 7690845. [CrossRef]
92. Kang, D.; Zuo, W.; Wu, Q.; Zhu, Q.; Liu, P. Inhibition of Specificity Protein 1 Is Involved in Phloretin-Induced Suppression of Prostate Cancer. *Biomed. Res. Int.* **2020**, *2020*, 1358674. [CrossRef]
93. Aggarwal, V.; Tuli, H.S.; Kaur, J.; Aggarwal, D.; Parashar, G.; Chaturvedi Parashar, N.; Kulkarni, S.; Kaur, G.; Sak, K.; Kumar, M.; et al. Garcinol Exhibits Anti-Neoplastic Effects by Targeting Diverse Oncogenic Factors in Tumor Cells. *Biomedicines* **2020**, *8*, 103. [CrossRef]
94. Yang, G.; Yin, X.; Ma, D.; Su, Z. Anticancer activity of Phloretin against the human oral cancer cells is due to G0/G1 cell cycle arrest and ROS mediated cell death—PubMed. *J. Buon.* **2020**, *25*, 344–349.
95. Roy, S.; Mondru, A.K.; Chakraborty, T.; Das, A.; Dasgupta, S. Apple polyphenol phloretin complexed with ruthenium is capable of reprogramming the breast cancer microenvironment through modulation of PI3K/Akt/mTOR/VEGF pathways. *Toxicol. Appl. Pharmacol.* **2022**, *434*, 115822. [CrossRef]
96. Kim, J.L.; Lee, D.H.; Pan, C.H.; Park, S.J.; Oh, S.C.; Lee, S.Y. Role of phloretin as a sensitizer to TRAIL-induced apoptosis in colon cancer. *Oncol. Lett.* **2022**, *24*, 321. [CrossRef]
97. Andreani, T.; Cheng, R.; Elbadri, K.; Ferro, C.; Menezes, T.; dos Santos, M.R.; Pereira, C.M.; Santos, H.A. Natural compounds-based nanomedicines for cancer treatment: Future directions and challenges. *Drug Deliv. Transl. Res.* **2024**, *14*, 2845–2916. [CrossRef]